

Stochastic resonance in a parallel array of nonlinear dynamical elements

Fabing Duan^{a,*}, François Chapeau-Blondeau^b, Derek Abbott^c

^a *Institute of Complexity Science, Qingdao University, Qingdao 266071, PR China*

^b *Laboratoire d'Ingénierie des Systèmes Automatisés (LISA), Université d'Angers, 62 avenue Notre Dame du Lac, 49000 Angers, France*

^c *Centre for Biomedical Engineering (CBME) and School of Electrical & Electronic Engineering, The University of Adelaide, Adelaide, SA 5005, Australia*

Received 24 April 2007; received in revised form 28 August 2007; accepted 12 October 2007

Available online 13 November 2007

Communicated by C.R. Doering

Abstract

In an uncoupled parallel array of bistable dynamical elements subject to a common noisy subthreshold rectangular signal, the signal-to-noise ratio (SNR) gain can be improved by tuning the internally added array noise. A SNR gain above unity is observed in certain regions of the array noise intensity. The maximum SNR gain is obtained as the size of the array goes to infinity. This form of stochastic resonance (SR), i.e., array SR, is analytically described by introducing a quasi-stationary probability density model, yielding expressions for the transition probability and the stationary autocorrelation function. The analytical results have interpretative value for the mechanism of array SR, and may be of heuristic interest for applying array SR to related signal processing problems. Additionally, the analytical descriptions of an isolated bistable system agree well with numerical results of both conventional SR for a subthreshold rectangular input and residual SR for a slightly suprathreshold signal.

© 2007 Elsevier B.V. All rights reserved.

Keywords: Array stochastic resonance; Signal-to-noise ratio gain; Dynamical subsystem; Array signal processing

1. Introduction

Stochastic resonance (SR) is an interesting nonlinear phenomenon where noise plays a constructive role in a variety of systems [1–7]. Now, SR research extends into interdisciplinary fields, involving physics, biology, neuroscience, and information processing [1–10]. Over time, the notion of SR has been widened to include a number of different mechanisms and new applications with novel types of SR having been discovered [1–21]. An originally theoretical description of the SR effect in a bistable system based on a two-state model was put forward by Nicolis [3]. Later, McNamara and Wiesenfeld used the output signal-to-noise ratio (SNR) metric for obtaining the signature of SR, i.e., a non-monotonic function of the background noise intensity [4]. Since then, the SNR is most frequently employed for studying conventional (periodic) SR effects in a nonlinear (static or dynamic) system driven by a subthreshold

periodic input. The SNR gain, defined as the ratio of the output SNR over the input SNR, attracts much interest in exploring situations where it can exceed unity [5–16]. Within the regime of validity of linear response theory, it has been repeatedly pointed out that the gain cannot exceed unity for a nonlinear system driven by a sinusoidal signal and Gaussian white noise [1,5,17,18]. However, beyond the regime where linear response theory applies, it has been demonstrated that the gain can indeed exceed unity in non-dynamical systems, such as a level-crossing detector [8], parallel arrays of threshold comparators or sensors [11,12], and also in bistable dynamical systems [7,9,13–16,19].

We have reported that SNR gain exceeding unity is achievable when a parallel array of bistable dynamical subsystems is subjected to a noisy subthreshold or suprathreshold sinusoid [19]. This result was first obtained in a parallel array of power-law sensors [11]. However, no theoretical explanation was given for the interesting numerical results presented in array of bistable dynamical subsystems [19]. In this Letter, our focus is on parallel arrays of bistable dynamical elements with a common noisy subthreshold rectangular input. Explicit expressions for the probability density, transition probability

* Corresponding author.

E-mail address: fabing1974@yahoo.com.cn (F. Duan).

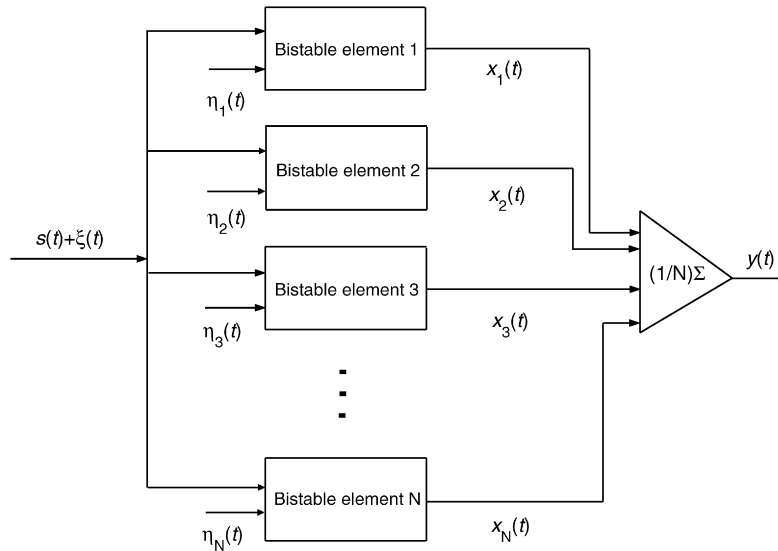


Fig. 1. A parallel array of N bistable elements. Each element is subject to the same noisy signal $s(t) + \xi(t)$ but independent array noise $\eta_i(t)$. The array output is $y(t) = \sum_{i=1}^N x_i(t)/N$. In this Letter, we call $\xi(t)$ the input noise and $\eta_i(t)$ the array noise.

and the stationary autocorrelation function will be deduced in the following. The analytical description for conventional SR agrees well with the numerical result for an isolated bistable system. It is also noted that residual SR [20] can be analytically well-described for a slightly suprathreshold input, while this Letter mainly focuses on how to improve the SNR gain of the subthreshold input signals. To do this, the array noise is tuned and the array SR effect is utilized. The positive role of moderate array noise is to help the array output evolve dominantly at the same period as the input, whereas too much noise is deleterious—playing a negative role (see Section 2). Fortunately, this negative role can be weakened by increasing the array size, and entirely eliminated for an infinite array. As a consequence, the SNR and the SNR gain can be analytically expressed as functions of the array noise intensity. This theory of array SR analytically describes the array SR phenomenon, and demonstrates the SNR gain exceeding unity. The validity of array SR theory is discussed and further studies need to be developed.

The proposed array SR theory indicates that an uncoupled parallel array of bistable dynamical subsystems constructs a meaningful collective device for amplifying the statistical measure of the SNR. Therefore, we argue that this leads to new promising applications in array signal processing that deserve to be studied.

2. The model and the array SR theory

An uncoupled parallel array of N archetypal over-damped bistable elements is considered as a block diagram, as shown in Fig. 1. Each bistable element is subject to the same signal-plus-noise mixture $s(t) + \xi(t)$, where $s(t) = A$ ($s(t) = -A$) if $t \in [nT_s/2, (n+1)T_s/2]$ with n even (odd). In other words, $s(t)$ is a periodic rectangular signal. Here, $\xi(t)$ is zero-mean Gaussian white noise, independent of $s(t)$, with autocorrelation $\langle \xi(t)\xi(0) \rangle = 2D_\xi \delta(t)$ and noise intensity D_ξ . At the same time,

zero-mean Gaussian white noise $\eta_i(t)$, together with and independent of $s(t) + \xi(t)$, is applied to each element of the parallel array of size N . The N array noise terms $\eta_i(t)$ are mutually independent and have autocorrelation $\langle \eta_i(t)\eta_i(0) \rangle = 2D_\eta \delta(t)$ with a same noise intensity D_η [11,12,19]. The internal state $x_i(t)$ of each dynamic bistable element is governed by

$$\tau_a \frac{dx_i(t)}{dt} = x_i(t) - \frac{x_i^3(t)}{X_b^2} + s(t) + \xi(t) + \eta_i(t), \quad (1)$$

for $i = 1, 2, \dots, N$. Their outputs, as shown in Fig. 1, are averaged and the response of the array is given as

$$y(t) = \frac{1}{N} \sum_{i=1}^N x_i(t). \quad (2)$$

Here, the real tunable array parameters τ_a and X_b are in the dimensions of time and amplitude, respectively [21]. We now rescale the variables according to

$$\begin{aligned} x_i(t)/X_b &\rightarrow x_i(t), & A/X_b &\rightarrow A, \\ D_\eta/(\tau_a X_b^2) &\rightarrow D_\eta, & t/\tau_a &\rightarrow t, \\ T_s/\tau_a &\rightarrow T_s, & D_\xi/(\tau_a X_b^2) &\rightarrow D_\xi, \end{aligned} \quad (3)$$

where each arrow points to a dimensionless variable. Eq. (1) is then recast in a dimensionless form as

$$\frac{dx_i(t)}{dt} = x_i(t) - x_i^3(t) + s(t) + \xi(t) + \eta_i(t). \quad (4)$$

Note that $s(t)$ is subthreshold if the dimensionless amplitude $A < A_c = 2/\sqrt{27} \approx 0.385$, and suprathreshold otherwise [7,13,21].

2.1. Quasi-stationary probability density and the non-stationary mean function

In each half period of $T_s/2$, the statistically equivalent description for the corresponding probability density $\rho(x, t)$ is

governed by the Fokker–Planck equation

$$\frac{\partial \rho(x, t)}{\partial t} = L_{\text{FP}} \rho(x, t), \quad (5)$$

where the Fokker–Planck operator $L_{\text{FP}} = -\partial(x - x^3 \pm A)/\partial x + D\partial^2/\partial x^2$ and $D = D_\xi + D_\eta$. The steady-state solution of Eq. (5), for a constant input at $\pm A$, is given by

$$\rho_{\pm A} = \lim_{t \rightarrow \infty} \rho(x, t) = C e^{-\Phi(x)}, \quad (6)$$

where C is the integration constant, which has to be chosen such that $\rho_{\pm A}$ is normalized [27]. In Eq. (6) we introduce the potential $\Phi(x) = -(x^2/2 - x^4/4 \pm Ax)/D$ [27]. Assume that $\rho(x, t)$ obeys natural boundary conditions such that it vanishes at large x for any t . We have expanded probability density $\rho(x, t)$ as

$$\rho(x, t) = \sum_n c_n \psi_n(x) e^{-\frac{\Phi(x)}{2}} e^{-\lambda_n t}, \quad (7)$$

where the constant coefficients c_n can be calculated by inserting the initial conditions [21–23]. Here, we assume $\phi_n(x)$ as the eigenfunctions of L_{FP} with discrete eigenvalues λ_n ($n = 0, 1, \dots$), and the functions $\psi_n(x) = \phi_n(x) e^{\frac{\Phi(x)}{2}}$ are the eigenfunctions of Hermitian operator $L = e^{-\frac{\Phi(x)}{2}} L_{\text{FP}} e^{\frac{\Phi(x)}{2}}$ with the same eigenvalues λ_n . The positivity of eigenvalues $\lambda_0 = 0 < \lambda_1 < \dots < \lambda_n < \dots$ has been demonstrated [21–23].

Next, we take the first two terms of Eq. (7) as a simple quasi-stationary probability distribution model [21–23]. Then, if the preceding input signal amplitude is $s(t) = \mp A$ and the next one is $s(t) = \pm A$, the quasi-stationary probability distribution model is derived as

$$\rho(x, t)_{\pm A} \approx \rho_{\pm A} + [\rho_{\mp A} - \rho_{\pm A}] e^{-\lambda_1 t}, \quad (8)$$

with the initial condition $\rho(x, t = 0)_{\pm A} = \rho_{\mp A}$ and stationary condition $\rho(x, t = +\infty)_{\pm A} = \rho_{\pm A}$ [21–23]. In one period T_s , we use $\rho(x, t)_{+A}$ for a positive square waveform during $[0, T_s/2]$ and $\rho(x, t)_{-A}$ for a negative one in $[T_s/2, T_s]$. This assumption is built on the fact that the system can almost reach the stationary probability density $\rho_{\pm A}$ in half period $T_s/2$, if the lowest positive eigenvalue λ_1 is much larger than the signal frequency $1/T_s$, as shown in Fig. 2. Especially worthy of note is the lowest positive eigenvalue, λ_1 , which describes the main speed of $\rho(x, t)$ of Eq. (8) tending to the stationary solution of Eq. (6).

Now, we introduce the function $n(t) = \lfloor 2t/T_s \rfloor$, $\lfloor z \rfloor$ being the floor function of z , i.e., the greatest integer less than or equal to z [13]. Then, the quasi-stationary probability density can be expressed as

$$\rho(x, t)_{(-1)^{n(t)}A} = \rho_{(-1)^{n(t)}A} + e^{-\lambda_1(t - \frac{n(t)T_s}{2})} \times [\rho_{(-1)^{1+n(t)}A} - \rho_{(-1)^{n(t)}A}], \quad (9)$$

and the non-stationary mean function is given by

$$E[x(t)] = \int_{-\infty}^{+\infty} x \rho(x, t)_{(-1)^{n(t)}A} dx. \quad (10)$$

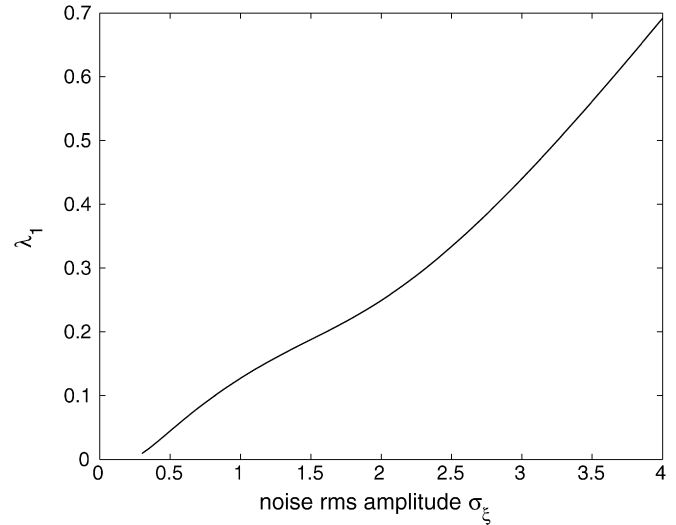


Fig. 2. The lowest positive eigenvalue of λ_1 as a function of input noise rms amplitude σ_ξ . Here, $A = 0.34$, $T_s = 100$ and $\Delta t = 0.1$.

We emphasize that Eqs. (7)–(9) are a new version of a Floquet-like analysis and a general Floquet-type depiction has been reported by Jung [6]. In this Letter, the non-Hermitian operator L_{FP} is transformed into an Hermitian operator L . As a consequence, the eigenvalues λ_n are in general real-valued quantities. However, the extended periodic Fokker–Planck operator is usually a non-Hermitian operator with complex Floquet eigenvalues [6]. Another difference is that the variational method is used for numerically determining the lowest positive eigenvalue [21,22], while the matrix continued fraction method is appropriate for solving all eigenvalues and eigenfunctions [6,27]. We recognize that the lowest positive eigenvalue introduced here, similar to the smallest non-vanishing real eigenvalue in [6], is an important quantity representing the system relaxation time scale. The general Floquet theory is an adequate mathematical tool for periodically driven stochastic systems [1,6]. Our analysis is a particular line of research building on preceding results [11,12,19].

2.2. Stationary auto-covariance function and the SNR gain

In this subsection, we take the output of bistable system as a Markov process [27]. Note that the transition probability $P(x, t|x', t')$ fulfils the initial condition $\lim_{t \rightarrow t'} P(x, t|x', t') = \delta(x - x')$, since the time difference $t - t'$ of the transition probability $P(x, t|x', t')$ of Markov process is arbitrary [27, 28]. If the signal amplitude keeps $\pm A$ for $t \rightarrow +\infty$, the transition probability then satisfies the stationary condition $\lim_{t \rightarrow +\infty} P(x, t|x', t') = \rho_{(-1)^{n(t)}A}$. Moreover, the completeness relation for the eigenfunctions ψ_n and ϕ_n can be expressed as $\delta(x - x') = \sum_n \psi_n(x)\psi_n(x') = e^{\Phi(x')} \sum_n \phi_n(x)\phi_n(x')$ [27]. Thus, the transition probability can be expanded into eigenfunctions [27]

$$\begin{aligned} P(x, t|x', t') &= e^{L_{\text{FP}}(x)(t-t')} \delta(x - x') \\ &= e^{\Phi(x')} \sum_n \phi_n(x)\phi_n(x') e^{-\lambda_n(t-t')} \end{aligned}$$

$$= \psi_0(x)\psi_0^{-1}(x') \\ \times \sum_n \psi_n(x)\psi_n(x')e^{-\lambda_n(t-t')}.$$

As the treatment of the quasi-stationary probability distribution model of Eq. (8), we similarly truncate the expansion of $P(x, t|x', t')$ with the first two terms, and utilize the zero eigenvalue λ_0 and the first positive one λ_1 . With the above initial and stationary conditions, the transition probability is derived as

$$P(x, t|x', t') = \rho(x, t)_{(-1)^{n(t)}A} + \delta(x - x') \\ \times [1 - \rho(x', t')_{(-1)^{n(t')}A}]e^{-\lambda_1|t-t'|}.$$

Considering the input rectangular signal, we assume the transition probability $P(x, t|x', t')$ is sufficiently small between the timescale $t \in [(n-1)T_s/2, nT_s/2]$ and $t \in [nT_s/2, (n+1)T_s/2]$. This assumption is coincident with the fact of the eigenvalue λ_1 being larger than $1/T_s$ in resonant region of noise intensity, as shown in Figs. 2 and 3. The transition probability is then expressed as

$$P(x, t|x', t') = \rho(x, t)_{(-1)^{n(t)}A} + \delta(x - x') \\ \times [\delta(n(t) - n(t')) - \rho(x', t')_{(-1)^{n(t')}A}] \\ \times e^{-\lambda_1|t-t'|}, \quad (11)$$

and the two-time joint probability density can be derived as

$$\rho(x, t|x', t') = P(x, t|x', t')\rho(x', t')_{(-1)^{n(t')}A}. \quad (12)$$

The expectation

$$E[x(t)x(t+\tau)] = \iint xy\rho(y, t+\tau|x, t) dx dy \\ = [E[x^2(t)] - E^2[x(t)]]e^{-\lambda_1|\tau|} \\ + E[x(t)]E[x(t+\tau)], \quad (13)$$

is periodic in t with period T_s [10]. Then, we construct the stationary auto-covariance function as

$$C_{xx}(\tau) = \langle E[x(t+\tau)x(t)] - E[x(t)]E[x(t+\tau)] \rangle \\ = \langle E[x^2(t)] - E^2[x(t)] \rangle e^{-\lambda_1|\tau|}, \quad (14)$$

where $\langle \dots \rangle = \frac{1}{T_s} \int_0^{T_s} \dots dt$.

Now, we can theoretically calculate the non-stationary mean function $E[x(t)]$, i.e., Eq. (10) and the stationary auto-covariance function $C_{xx}(\tau)$, i.e., Eq. (14). Then, we have the order n Fourier coefficient of $E[x(t)]$

$$\bar{Y}_n = \langle E[x(t)]e^{-i2\pi \frac{n}{T_s}t} \rangle, \quad (15)$$

and the Fourier transform of $C_{xx}(\tau)$ as

$$P_{\text{noise}}(\nu) = \int_{-\infty}^{+\infty} C_{xx}(\tau)e^{-i2\pi\nu\tau} d\tau \\ = \langle E[x^2(t)] - E^2[x(t)] \rangle \frac{2\lambda_1}{\lambda_1^2 + \nu^2}. \quad (16)$$

Thus, the output SNR is the power contained in the output spectral line $1/T_s$ divided by the power contained in the noise

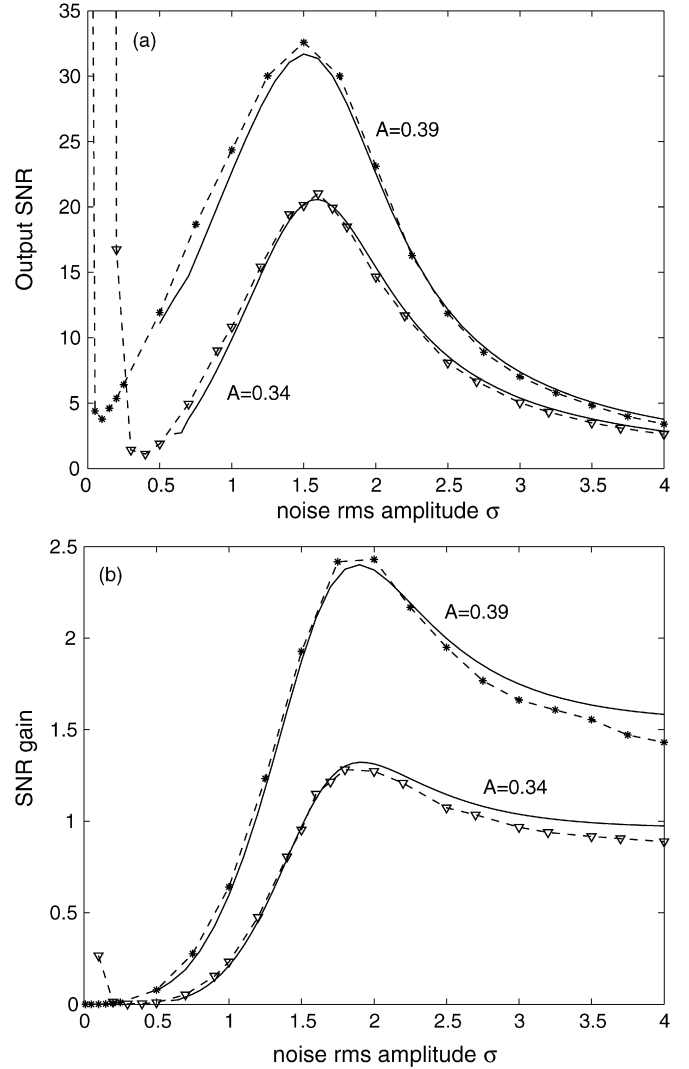


Fig. 3. The conventional SR phenomenon in the isolated bistable element of Eq. (4) in the absence of array noise. Here, $A = 0.34$ (∇ , subthreshold) or 0.39 ($*$, slightly suprathreshold), $T_s = 100$, $\Delta t = 0.1$ and $\Delta t \Delta B = 10^{-3}$. (a) The output SNR $R_{\text{out}}(1/T_s)$ as a function of σ_ξ , i.e., the rms amplitude of input noise $\xi(t)$. (b) The SNR gain G as a function of σ_ξ . The solid lines depict the theoretical results of Eq. (18), whereas the numerical results are given by the dashed lines.

background in a small frequency bin $\Delta B = 1/T_s$ around $1/T_s$, i.e.,

$$R_{\text{out}}(1/T_s) = \frac{|\bar{Y}_1|^2}{P_{\text{noise}}(1/T_s)\Delta B} \\ = \frac{|\bar{Y}_1|^2[\lambda_1^2 + (1/T_s)^2]}{2\langle E[x^2(t)] - E^2[x(t)] \rangle \lambda_1 \Delta B}. \quad (17)$$

Here, the signal-plus-noise mixture of $s(t) + \xi(t)$ is initially given, and the theoretical expression for input SNR can be computed as $R_{\text{in}}(1/T_s) = 4A^2/(2\pi^2 D_\xi \Delta B)$, we then have the SNR gain

$$G = \frac{R_{\text{out}}(1/T_s)}{R_{\text{in}}(1/T_s)} \\ = \frac{|\bar{Y}_1|^2[\lambda_1^2 + (1/T_s)^2]}{\langle E[x^2(t)] - E^2[x(t)] \rangle \lambda_1} \frac{D_\xi}{4A^2/\pi^2}. \quad (18)$$

In the discrete-time implementation of the process, the sampling time $\Delta t \ll T_s$ and τ_a . The incoherent statistical fluctuations in the input $s(t) + \xi(t)$, which control the continuous noise background in the input power spectral density, are measured by the variance $\sigma_\xi^2 = 2D_\xi/\Delta t$ [10]. Here, σ_ξ is the rms amplitude of input noise $\xi(t)$, and the rms amplitude of array noise $\eta_i(t)$ is σ_η . The numerical method for calculating SNR and SNR gain is introduced in Appendix A. If array noise $\eta_i(t)$ is absent in Eq. (4), this model of Eq. (4) is identical with an isolated bistable system studied in [1,13]. The conventional SR effect can be viewed as a non-monotonic evolution of the output SNR with the rms amplitude of the input noise $\xi(t)$. The theoretical results obtained from Eq. (18) agree well with the numerical data, as shown in Fig. 3(a). It is worthy of note that the residual SR of a slightly suprathreshold input can also be theoretically well-described. The SNR gain, as illustrated in Fig. 3(b), is beyond unity at a certain range of σ_ξ . This conclusion is consistent with the work of Refs. [7,9,13–15].

We should note that the smallest non-vanishing eigenvalue λ_1 of the Fokker–Planck operator can be approximated with a very high accuracy and some simple asymptotic equations were extensively developed in the pioneering research work [1,6,24–26]. Thus, the analytic results of the present Letter can be simplified by using these available expressions of λ_1 . This Letter, however, provides an important evolution of our previous work [21–23], and a general solution method for theoretically describing SR effects in the bistable systems. More interesting is that this general solution method can describe residual SR phenomenon well, and highlight a theoretical view on the mechanism of array SR in the parallel array of bistable subsystems as follows.

2.3. Theory of array SR

In an isolated bistable system, the SNR gain G follows a non-monotonic curve as σ_ξ increases. The maximum SNR gain G is about 1.3 for the subthreshold input signal given in Fig. 3. Now, an interesting question arises, namely, can we further improve the SNR gain? The answer is positive and lies in the operation of array SR [11,12,19].

In the presence of array noise $\eta_i(t)$, the parallel array of bistable elements of Eq. (4) can demonstrate the SR phenomenon for both subthreshold and suprathreshold sinusoids [19]. In the present Letter, a noisy subthreshold rectangular signal is employed resulting in tractable analytical descriptions of array SR and SNR gain.

At any time t , we express the random output $x_i(t)$ as the sum of its non-stationary mean $E[x_i(t)]$, plus the statistical fluctuations $\tilde{x}_i(t)$ induced by $\xi(t) + \eta_i(t)$ around the mean, i.e.

$$x_i(t) = \tilde{x}_i(t) + E[x_i(t)], \quad (19)$$

for $i = 1, 2, \dots, N$. As discussed in [19], the stationary autocovariance function $C_{yy}(\tau)$ of the parallel array with size N can be expressed as

$$C_{yy}(\tau) = \langle E[y(t)y(t+\tau)] - E[y(t)]E[y(t+\tau)] \rangle$$

$$\begin{aligned} &= \langle E[x_i(t)x_j(t+\tau)] - E[x_i(t)]E[x_j(t+\tau)] \rangle \\ &\quad + \frac{\langle E[x_i(t)x_i(t+\tau)] - E[x_i(t)]E[x_i(t+\tau)] \rangle}{N} \\ &= \langle E[\tilde{x}_i(t)\tilde{x}_j(t+\tau)] \rangle \\ &\quad + \frac{\langle E[\tilde{x}_i(t)\tilde{x}_i(t+\tau)] - E[\tilde{x}_i(t)]E[\tilde{x}_i(t+\tau)] \rangle}{N}, \quad (20) \end{aligned}$$

for $i \neq j$ and $i, j = 1, 2, \dots, N$. Note that $E[x_i(t)] = E[x_j(t)]$.

When array size $N = 1$, Eq. (20), i.e., $C_{yy}(\tau) = \langle E[\tilde{x}_i(t)\tilde{x}_i(t+\tau)] \rangle$ reduces to $C_{x_i x_i}(\tau)$ defined in Eq. (14). It is seen in Eq. (20) that as the array size N ($N > 1$) increases, the variance of $E[\tilde{x}_i(t)\tilde{x}_i(t+\tau)] - E[\tilde{x}_i(t)]E[\tilde{x}_i(t+\tau)]$ decreases at a rate of $1/N$. In other words, the negative influence of $E[\tilde{x}_i(t)\tilde{x}_i(t+\tau)] - E[\tilde{x}_i(t)]E[\tilde{x}_i(t+\tau)]$ can be weakened by the array size N . If the array size $N = +\infty$ and $i \neq j$, $E[\tilde{x}_i(t)\tilde{x}_i(t+\tau)] - E[\tilde{x}_i(t)]E[\tilde{x}_i(t+\tau)]$ is totally eliminated [19]. In this case, Eq. (20) becomes

$$\lim_{N \rightarrow \infty} C_{yy}(\tau) = C_{x_i x_j} = \langle E[\tilde{x}_i(t)\tilde{x}_j(t+\tau)] \rangle. \quad (21)$$

Since the indices i and j are different, but arbitrary in Eqs. (20) and (21), we can take two bistable elements, each embedded with independent array noise, to evaluate the SNR gain of a parallel array with size $N > 1$. This method is tractable and effective [19], as shown in Fig. 4(a).

The nonlinear characteristics of the array interact with input noise $\xi(t)$ and array noise $\eta_i(t)$. This point makes it very difficult to calculate the stationary autocovariance function of $C_{x_i x_i} = \langle E[\tilde{x}_i(t)\tilde{x}_i(t+\tau)] \rangle$ and the stationary covariance function of $C_{x_i x_j} = \langle E[\tilde{x}_i(t)\tilde{x}_j(t+\tau)] \rangle$. A visible fact, as shown in Fig. 4(a), is that $C_{x_i x_j} = C_{x_i x_i}$ at $D_\eta = 0$. Upon combining Eq. (14), we assume

$$\begin{aligned} C_{x_i x_j}(\tau) &= \frac{D_\xi}{D} C_{x_i x_i}(\tau) \\ &= \frac{D_\xi}{D} \langle E[x_i^2(t)] - E^2[x_i(t)] \rangle e^{-\lambda_1|\tau|}, \quad (22) \end{aligned}$$

with a supposed coefficient $D_\xi/D = D_\xi/(D_\xi + D_\eta)$. This simple coefficient is not involved in the interaction of input noise $\xi(t)$ and array noise $\eta_i(t)$. In this way, Eq. (20) can be represented as

$$\begin{aligned} C_{yy}(\tau) &= C_{yy}(0)h(\tau) \\ &= \langle E[x_i^2(t)] - E^2[x_i(t)] \rangle e^{-\lambda_1|\tau|} \\ &\quad \times \left(\frac{D_\xi}{D} + \frac{D_\eta}{ND} \right), \quad (23) \end{aligned}$$

with the stationary variance of $y(t)$, i.e., $C_{yy}(0) = [D_\xi/D + D_\eta/(ND)] \langle E[x_i^2(t)] - E^2[x_i(t)] \rangle$, and the correlation coefficient $h(\tau) = C_{yy}(\tau)/C_{yy}(0) = e^{-\lambda_1|\tau|}$. The output noise is assumed to be a Lorentz-like colored noise with the correlation time τ_r defined by $h(|\tau| \geq \tau_r) \leq 0.05$. Then, from Eqs. (14)–(23), we can theoretically evaluate the SNR gain obtained by array SR effects as

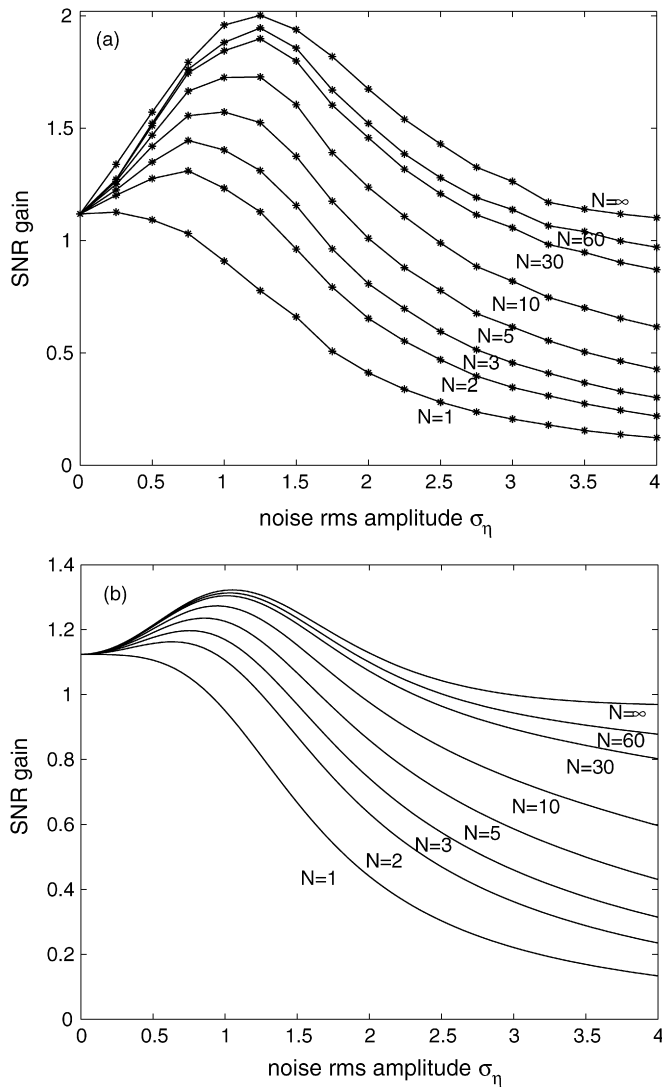


Fig. 4. Numerical (a) and theoretical (b) SNR gain as a function of the rms amplitude σ_η of array noise $\eta_i(t)$ for $A = 0.34$. The array SNR gain curves, from the bottom up, correspond to $N = 1, 2, 3, 5, 10, 30, 60, \infty$. The input noise rms amplitude $\sigma_\xi = 1.6$, and the given input SNR $R_{\text{in}} = 18.30$. Here, $T_s = 100$, $\Delta t \Delta B = 10^{-3}$, and $\Delta t = 0.1$.

$$G_{\text{array}} = \frac{|\bar{Y}_1|^2 [\lambda_1^2 + (1/T_s)^2]}{\langle E[x^2(t)] - E^2[x(t)] \lambda_1} \frac{D_\xi}{4A^2/\pi^2} \times \frac{D}{D_\xi + \frac{D_\eta}{N}} = \frac{GD}{D_\xi + \frac{D_\eta}{N}}, \quad (24)$$

for $N = 1, 2, \dots, \infty$.

Fig. 4 shows the numerical and theoretical behaviors of SNR gain obtained by tuning array noise rms amplitude σ_η . The input noise rms amplitude $\sigma_\xi = 1.6$. The local SNR gain is about 1.1 and the maximum SNR gain is about 1.3 for a subthreshold input, as shown in Fig. 3. Upon increasing σ_η , it is observed that the SNR gain can be improved further, and the numerical maximum SNR gain $G = 2.01$ occurs at $\sigma_\eta = 1.25$ and $N = \infty$, as shown in Fig. 4(a). This form of array SR effect in a dynamical array can be also demonstrated by the analytical description of Eqs. (14)–(24), as plotted out in Fig. 4(b). The observable quantitative discrepancies between the analytical results and numer-

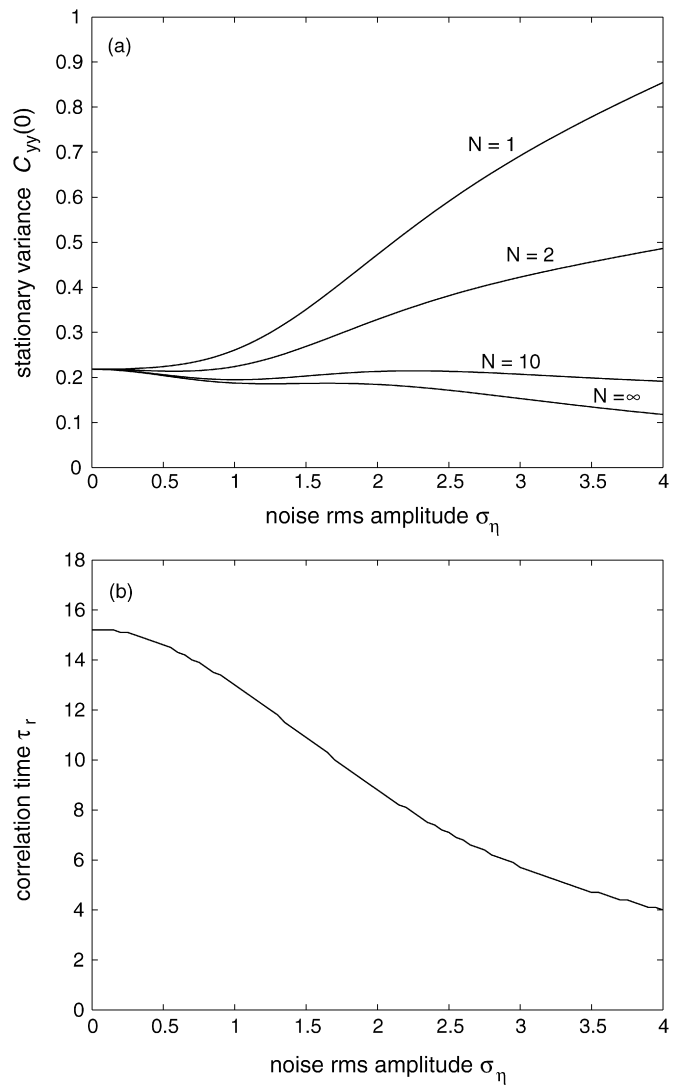


Fig. 5. Theoretical results of (a) the stationary variance $C_{yy}(0)$ and (b) the correlation time τ_r as a function of the rms amplitude σ_η of array noise $\eta_i(t)$ for $A = 0.34$. Note that the correlation time τ_r is the same for $N = 1, 2, \dots, \infty$. Other parameters are the same as in Fig. 4.

ical simulations are presented. The value of $1/\lambda_1$ decreases as the noise rms amplitude increases, as shown in Fig. 2. The addition of array noise $\eta_i(t)$ makes $1/\lambda_1$ smaller and smaller, relative to T_s . It is shown in Fig. 4 that the theoretical approximation is good if σ_η is in the regime close to 4. This is a key point for the range of validity of this theory. The array SR effect appears as the tuned array noise makes the array output evolve dominantly at the same period as the input. Fig. 5 shows the nonlinear behaviors of the stationary variance $C_{yy}(0)$ and the correlation time τ_r as a function of the rms amplitude σ_η . For array size $N = 1$, $C_{yy}(0)$ will increase as σ_η does, but the correlation function of $h(\tau)$ will have a shorter and shorter correlation time τ_r . Thus, the array noise $\eta_i(t)$ will “white” the output background noise with reduced τ_r . Due to the array size, as shown in Fig. 5(a), $C_{yy}(0)$ can be decreased to a limited value of $C_{yy}(0) = C_{x_i x_j}(0)$ for $N = \infty$. This indicates that the negative role of $\eta_i(t)$ can be counteracted by array size N . These aspects lead to the appearance of array SR, as seen in Fig. 4.

Moreover, the array SR region of array noise rms amplitude σ_η agrees well with the numerical results, as shown in Fig. 4. Thus, this array SR theory captures well both the non-monotonic behavior of SNR gain and the proper array SR region of array noise intensity. In practice, the inherent noise $\xi(t)$ might be unavoidable and embedded into the input signal. If the input noise rms amplitude σ_ξ is located at the left side of the SR peak, as shown in Fig. 3, the conventional SR method of adding more noise can reach the SR peak and obtain the maximum SNR gain about 1.3 for a subthreshold input. However, if the input noise rms amplitude σ_ξ is located at the right side of the SR peak, the addition of noise is of no use via conventional SR [23]. In this case, the array noise $\eta_i(t)$ can be tuned appropriately for obtaining a higher SNR gain via array SR, as shown in Fig. 4. The array SR theory then tells us the appropriate amount of array noise to be added to the parallel array of bistable elements.

3. Conclusion

We studied array SR in an uncoupled parallel array of bistable elements subject to an identical noisy subthreshold rectangular signal. We explicitly expressed the non-stationary mean function, the stationary autocorrelation function, and the output SNR of the array response. The agreement between the analytical results and the numerical results is good for an isolated bistable system in the context of conventional SR or residual SR. The theoretical analysis of array SR does reproduce the bell-shaped resonant behavior of SNR vs array noise intensity, and the SNR gain exceeds unity for the appropriate range of array noise intensity. Finally, we point out that array SR can further improve the SNR gain, especially for larger noise and when the noise intensity is beyond the conventional SR region. This nonlinear collective characteristic of parallel dynamical arrays provides an efficient strategy for processing periodic signals. This analytical results exploits the extended SR mechanism in arrays of these type of dynamical subsystems, and provides a different mathematical approach for describing SR effects. An open problem, such as optimizing the maximum SNR gain, via tuning array parameters and array noise, is interesting and remains open for future research.

Acknowledgements

We gratefully thank the anonymous reviewers for their constructive comments and suggestions. This work is sponsored by NSFC (No. 60602040), Taishan Scholar CPSP, the SRF for ROCS, SEM and PhD PFME of China (No. 20051065002). Funding from the Australian Research Council (ARC) is gratefully acknowledged.

Appendix A. Numerical method of computing power spectra of the collective response of arrays

The corresponding measured power spectra of the collective response $y(t) = (1/N) \sum_{i=1}^N x_i(t)$ are computed in a numerical iterated process in the following way that is based on the

theoretical derivations contained in [10,12]. The total evolution time of Eq. (4) is $(K+1)T_s$, while the first period of data is discarded to skip the start-up transient [7]. In each period T_s , the time scale is discretized with a sampling time $\Delta t \ll T_s$ such that $T_s = L\Delta t$. The white noise is with a correlation duration much smaller than T_s and Δt . We choose a frequency bin $\Delta B = 1/T_s$, and we shall stick to $\Delta t\Delta B = 10^{-3}$, $T_s = 100$, $L = 1000$ and $K \geq 10^5$ in this Letter. In succession, we follow:

(a) The estimation of the mean $E[y(j\Delta t)]$ is obtained over one period $[0, T_s[$, and the precise time $j\Delta t$ of $E[y(j\Delta t)]$ ($j = 0, 1, \dots, L-1$) shall be tracked correctly in each periodic evolution of Eq. (4), i.e., $[kT_s, (k+1)T_s[$ for $k = 1, 2, \dots, K$.

(b) For a fixed time of $\tau = i\Delta t$, the products $y(j\Delta t) \times y(j\Delta t + i\Delta t)$ are calculated for $j = 1, 2, \dots, K T_s/\Delta t$. Here, $i = 0, 1, \dots, \tau_{\max}/\Delta t$. The estimation of the expectation $E[y(j\Delta t)y(j\Delta t + i\Delta t)]$ is then performed over a time domain $\tau \in [0, \tau_{\max}[$. Immediately, the stationary autocovariance function $C_{yy}(i\Delta t)$ of Eqs. (14) and (20) at $i = 0, 1, \dots, \tau_{\max}/\Delta t$ can be deduced. Note the time τ_{\max} is selected in such a way that at τ_{\max} , the stationary autocovariance function $C_{yy}(i\Delta t)$ in Eq. (14) has returned to zero. In practice, we can select a quite small positive real number ε , such as $\varepsilon = 10^{-5}$. If $C_{yy}(i\Delta t)/C_{yy}(0) \leq \varepsilon$, the above computation shall be ceased and the index i_{end} is found, leading to $\tau_{\max} = i_{\text{end}}\Delta t$.

(c) Upon increasing the total evolution time of Eq. (4) as $(K'+1)T_s$ ($K' > K$), and evaluate the mean $E'[y(j\Delta t)]$ and the stationary autocovariance function $C'_{yy}(i\Delta t)$ again. If the differences between $E'[y(j\Delta t)]$ and $E[y(j\Delta t)]$, $C'_{yy}[i\Delta t]$ and $C_{yy}(i\Delta t)$, converged within an allowable tolerance, we go to the next step (d). If they do not converge, the total evolution time of Eq. (4) should be increased to $(K''+1)T_s$ larger than $(K'+1)T_s$, until the convergence is realized.

(d) With the converged mean $E[y(j\Delta t)]$ and stationary autocovariance function $C_{yy}(i\Delta t)$, the corresponding Fourier coefficient \bar{Y}_1 and the power $P_{\text{noise}}(1/T_s)$ of Eq. (17) contained in the noise background around $1/T_s$ can be numerically developed. The ratio of above numerical values leads to the array SNR R_{out} . The correlation time $\tau_r = M\Delta t$ as $|h(M\Delta t)| = |C_{yy}(M\Delta t)/C_{yy}(0)| \leq 0.05$. The numerical input SNR R_{in} can be also calculated by following steps (a)–(d), and compared with the theoretical value of R_{in} . The SNR gain G_{array} will be finally determined by Eqs. (18) and (24).

References

- [1] L. Gammaitoni, P. Hänggi, P. Jung, F. Marchesoni, Rev. Mod. Phys. 70 (1998) 233.
- [2] R. Benzi, A. Sutera, A. Vulpiani, J. Phys. A: Math. Gen. 14 (1981) L453.
- [3] C. Nicolis, Tellus 34 (1982) 1.
- [4] B. McNamara, K. Wiensfeld, Phys. Rev. A 39 (1989) 4854.
- [5] P. Jung, P. Hänggi, Phys. Rev. A 44 (1991) 8032.
- [6] P. Jung, Phys. Rep. 234 (1993) 175.
- [7] P. Hänggi, M.E. Inchiosa, D. Fogliatti, A.R. Bulsara, Phys. Rev. E 62 (2000) 6155.
- [8] K. Loerincz, Z. Gingl, L.B. Kiss, Phys. Lett. A 224 (1996) 63.
- [9] Z. Gingl, P. Makra, R. Vajtai, Fluct. Noise Lett. 1 (2001) L181.
- [10] F. Chapeau-Blondeau, X. Godivier, Phys. Rev. E 55 (1997) 1478.
- [11] F. Chapeau-Blondeau, D. Rousseau, Phys. Rev. E 70 (2004) 060101(R).

- [12] F. Chapeau-Blondeau, D. Rousseau, *Phys. Lett. A* 351 (2006) 231.
- [13] J. Casado-Pascual, J. Gómez-Ordóñez, M. Morillo, *Phys. Rev. Lett.* 91 (2003) 210601.
- [14] J. Casado-Pascual, C. Denk, J. Gómez-Ordóñez, M. Morillo, *Phys. Rev. E* 67 (2003) 036109.
- [15] J. Casado-Pascual, J. Gómez-Ordóñez, M. Morillo, P. Hänggi, *Phys. Rev. E* 68 (2003) 061104.
- [16] J.M. Casado, J. Gómez-Ordóñez, M. Morillo, *Phys. Rev. E* 73 (2006) 011109.
- [17] M.I. Dykman, P.V.E. McClintock, *Nature* 391 (1998) 344.
- [18] A. Neiman, L. Schimansky-Geier, F. Moss, *Phys. Rev. E* 56 (1997) R9.
- [19] F. Duan, F. Chapeau-Blondeau, D. Abbott, *Electron. Lett.* 42 (2006) 1008.
- [20] F. Apostolico, L. Gammaitoni, F. Marcheson, S. Santucci, *Phys. Rev. E* 55 (1997) 36.
- [21] F. Duan, D. Rousseau, F. Chapeau-Blondeau, *Phys. Rev. E* 69 (2004) 011109.
- [22] B. Xu, F. Duan, R. Bao, J. Li, *Chaos Solitons Fractals* 13 (2002) 633.
- [23] B. Xu, F. Duan, F. Chapeau-Blondeau, *Phys. Rev. E* 69 (2004) 061110.
- [24] R.S. Larson, M.D. Kostin, *J. Chem. Phys.* 69 (1978) 4821.
- [25] K. Schulten, Z. Schulten, A. Szabo, *J. Chem. Phys.* 74 (1981) 4426.
- [26] A. Perico, R. Pratolongo, K.F. Freed, R.W. Pastor, A. Szabo, *J. Chem. Phys.* 98 (1993) 564.
- [27] H. Risken, *The Fokker–Planck Equation: Methods of Solution and Applications*, second ed., Springer Series in Synergetics, vol. 18, Springer-Verlag, Berlin, 1989.
- [28] J. Mathews, R.L. Walker, *Mathematical Methods of Physics*, Benjamin, Menlo Park, CA, 1973.